Journal of Vertebrate Paleontology
Publication details, including instructions for authors and subscription information:
http://www.tandfonline.com/loi/ujvp20

Osteology, ontogeny, and phylogenetic position of Sinophoneus yumenensis (Therapsida, Dinocephalia) from the Middle Permian Dashankou Fauna of China

Jun Liu [a]

[a] Key Laboratory of Vertebrate Evolution and Human Origins of Chinese Academy of Sciences , Institute of Vertebrate Paleontology and Paleoanthropology, Chinese Academy of Sciences , 142 Xizhimenwai Street, Beijing , 100044 , China

Published online: 12 Nov 2013.

To cite this article: Jun Liu (2013) Osteology, ontogeny, and phylogenetic position of Sinophoneus yumenensis (Therapsida, Dinocephalia) from the Middle Permian Dashankou Fauna of China, Journal of Vertebrate Paleontology, 33:6, 1394-1407, DOI: 10.1080/02724634.2013.781505

To link to this article: http://dx.doi.org/10.1080/02724634.2013.781505

Journal of Vertebrate Paleontology 33(6):1394–1407, November 2013

ARTICLE

OSTEOLOGY, ONTOGENY, AND PHYLOGENETIC POSITION OF *SINOPHONEUS YUMENENSIS* (THERAPSIDA, DINOCEPHALIA) FROM THE MIDDLE PERMIAN DASHANKOU FAUNA OF CHINA

JUN LIU
Key Laboratory of Vertebrate Evolution and Human Origins of Chinese Academy of Sciences, Institute of Vertebrate Paleontology and Paleoanthropology, Chinese Academy of Sciences, 142 Xizhimenwai Street, Beijing, 100044, China, liujun@ivpp.ac.cn

ABSTRACT—*Sinophoneus yumenensis* and *Stenocybus acidentatus* are the only dinocephalians from China, and the latter taxon has been proposed to be a junior synonym of the former. Here I confirm this synonymy on the grounds that the differences between the two putative taxa are due to ontogenetic variation. The osteology of *Sinophoneus yumenensis* is described in detail based on both previously described specimens and several new ones from the same locality. *Sinophoneus yumenensis* differs from all other anteosaurs in having premaxillary dorsal processes that are separated by relatively long nasal anteromedial processes, and vomers without raised, elongated edges; from all other anteosaurs except *Archaeosyodon praeventor* in having distinct frontal posterolateral processes, and a wide intertemporal region formed partly by long posterior processes of the postfrontals that approach the posterior edge of the skull roof; and from *Archaeosyodon praeventor* in having a well-developed midline ridge on skull roof. A revised phylogenetic analysis including the new material recovers *Sinophoneus* as the most basal known anteosaurid.

SUPPLEMENTAL DATA—Supplemental materials are available for this article for free at www.tandfonline.com/UJVP

INTRODUCTION

Dinocephalians are a group of medium- to large-sized therapsids that have long been known from the Permian of Russian and South Africa. The first putative Chinese dinocephalian was *Taihangshania imperfecta*, based on some isolated teeth from Jiyuan, Henan (Young, 1979). These specimens were subsequently reinterpreted as worn or digested pareiasaurian teeth (Sigogneau-Russell and Sun, 1981). In the 1990s, two dinocephalian species were reported from Dashankou, Yumen, Gansu: *Sinophoneus yumenensis* (Cheng and Ji, 1996) and *Stenocybus acidentatus* (Li et al., 1996; Cheng and Li, 1997). The holotype of *Sinophoneus* (GMV 1601) represents a large animal, with a basal skull length of nearly 32 cm, whereas *Stenocybus* is much smaller with a basal skull length of about 12 cm. *Sinophoneus* was referred to Anteosauridae and suggested to be a close relative of *Titanophoneus* (Cheng and Ji, 1996). By contrast, *Stenocybus* was proposed to be the basal-most known dinocephalian, and used as the basis for the putative family Stenocybusidae (Cheng and Li, 1997). Ivakhnenko (1999, 2003) suggested that *Stenocybus* could represent a juvenile form of *Sinophoneus*. Recently, Kammerer (2011) formally proposed this synonymy, and showed that the phylogenetic position of *Sinophoneus* varies depending on how the ontogenetically variable characters in the analysis were scored.

In recent years, new dinocephalian specimens have been recovered from Brazil (Langer, 2000; Cisneros et al., 2012), Zimbabwe (Lepper et al., 2000), and Tanzania (Simon et al., 2010). However, these recent finds, with the exception of that reported by Cisneros et al. (2012), are fragmentary. Recently, new dinocephalian material from Dashankou has been collected and dinocephalians are now known to be abundant in the Dashankou Fauna (Li, 2001). Accordingly, the present study benefited from the availability of several new dinocephalian specimens, including seven nearly complete skulls associated with lower jaws. Our study of these dinocephalian specimens confirms that *Stenocybus acidentatus* is a synonym of *Sinophoneus yumenensis*. The specimens also provide detailed information on the morphology of *Sinophoneus yumenensis*, and allow an ontogenetic series to be assembled for this species. They also shed light on the phylogenetic position of *Sinophoneus yumenensis* within anteosaurids.

Institutional Abbreviations—**GMV**, Geological Museum of China, Beijing, China; **IGCAGS**, Institute of Geology, Chinese Academy of Geological Sciences, Beijing, China; **IVPP**, Institute of Vertebrate Paleontology and Paleoanthropology, Chinese Academy of Sciences, Beijing, China; **PIN**, Paleontological Institute of the Russian Academy of Sciences, Moscow, Russia.

Anatomical Abbreviations—**a**, angular; **art**, articular; **at.c**, atlas centrum; **at.n**, atlas neural arch; **ax.i**, axis intercentrum; **bo**, basioccipital; **bs**, basisphenoid; **c**, lower canine; **C**, upper canine; **cl**, clavicle; **cr**, coronoid; **ct**, cleithrum; **d**, dentary; **ec**, ectopterygoid; **eo**, exoccipital; **ep**, epipterygoid; **f**, frontal; **f.m**, foramen magnum; **i**, lower incisor; **I**, upper incisor; **icl**, interclavicle; **i.c**, foramen for internal carotid; **j**, jugal; **la**, lacrimal; **m**, maxilla; **n**, nasal; **p**, parietal; **pa**, proatlas; **pf**, postfrontal; **p.f**, pineal foramen; **pl**, palatine; **pm**, premaxilla; **po**, postorbital; **po.p**, paroccipital process; **poz**, postzygapophysis; **pp**, postparietal; **pra**, prearticular; **prf**, prefrontal; **pro**, prootic; **prz**, prezygapophysis; **ps**, parasphenoid; **pt**, pterygoid; **pt.f**, posttemporal fenestra; **q**, quadrate; **qj**, quadratojugal; **q.pt**, quadrate ramus of pterygoid; **sc**, scapula; **sm**, septomaxilla; **so**, supraoccipital; **sp**, splenial; **sq**, squamosal; **st**, stapes; **t**, tabular; **t.pt**, transverse process of pterygoid; **tr.p**, transverse process; **v**, vomer; **V**, vertebra.

SYSTEMATIC PALEONTOLOGY

THERAPSIDA Broom, 1905

DINOCEPHALIA Seeley, 1894

ANTEOSAURIA Boonstra, 1962
ANTEOSAURIDAE Boonstra, 1954
SINOPHONEUS YUMENENSIS Cheng and Ji, 1996
(Figs. 1–10)

Holotype—GMV 1601, a nearly complete skull missing the temporal arches.

Locality and Horizon—Dashankou, Yumen, Gansu Province, China; Qingtoushan Formation (formerly called the Xidagou Formation) (Liu et al., 2012).

Referred Specimens—IGCAGS V361, slightly damaged skull associated with almost complete lower jaws (holotype of *Stenocybus acidentatus*); IVPP V12008, right premaxilla, maxilla, and dentary with complete upper and lower dentitions (paratype of *Stenocybus acidentatus*); IVPP V18120, a slightly distorted skull with lower jaws and some postcranial elements; IVPP V18117–18119 and 18121–18123, six skulls with lower jaws; IVPP V18124, a nearly complete right dentary with 10 teeth; IVPP V18125, an incomplete left dentary with 14 teeth; IVPP V18126, an incomplete left maxilla with teeth; IVPP V18127, eight continuous presacral vertebrae with some ribs.

Diagnosis—*Sinophoneus yumenensis* can be distinguished from all other anteosaurs by the autapomorphic presence of premaxillary dorsal processes separated by relatively long nasal anteromedial processes, and of vomers without raised, elongated edges; from all other anteosaurs except *Archaeosyodon praeventor* by the presence of distinct frontal posterolateral processes and a wide intertemporal region formed partly by long posterior processes of the postfrontals that approach the posterior edge of the skull roof; and from *Archaeosyodon praeventor* by the presence of a well-developed midline ridge on the skull roof.

DESCRIPTION

All of the available skulls of *Sinophoneus yumenensis* are deformed to some degree, and not all of the specimens have been thoroughly prepared. However, most anatomical features can be observed in at least one of the available specimens. The holotype is relatively well preserved but shows almost no traceable sutures (Fig. 1). The following description draws information from all of the available specimens but is mainly based on the least distorted one, IVPP V18120 (Fig. 2).

The length of the skull from the tip of the snout to the occipital condyle ranges from approximately 12 to 32 cm (Table 1), but exceeds 18 cm only in the holotype. Among the available specimens, the smaller skulls are narrow and high (Figs. 3, 4), whereas the larger ones are relatively wider (Figs. 1, 2). The dorsal surface of the skull forms a triangular table, whereas the interorbital region is concave. Small specimens lack distinct pachyostosis, but the bones surrounding the orbit are pachyostosed in the holotype. The dorsal snout profile in lateral view is distinctly convex in small specimens, but relatively straight in large ones.

In absolute size, the external naris of the largest specimen is only slightly larger (Fig. 1) than that of the smallest one (Fig. 4), indicating that the relative size of this structure is greater in small specimens. In most specimens, the naris is located close to the ventral margin of the upper jaw, being separated from the premaxillary margin by a distance that is less than the height of the naris itself (Figs. 2–4). The holotype is the only known specimen in which the reverse is true.

The round orbit is quite large, measuring about double the area of the triangular temporal fenestra in small specimens (IVPP V18117, 18122) (Fig. 4), although the orbit appears smaller than the temporal fenestra in the holotype (Fig. 1). The temporal fenestra is semicircular, and its apex lies only slightly ventral to the level of the dorsal margin of the orbit. The intertemporal region is only slightly narrower than the interorbital region.

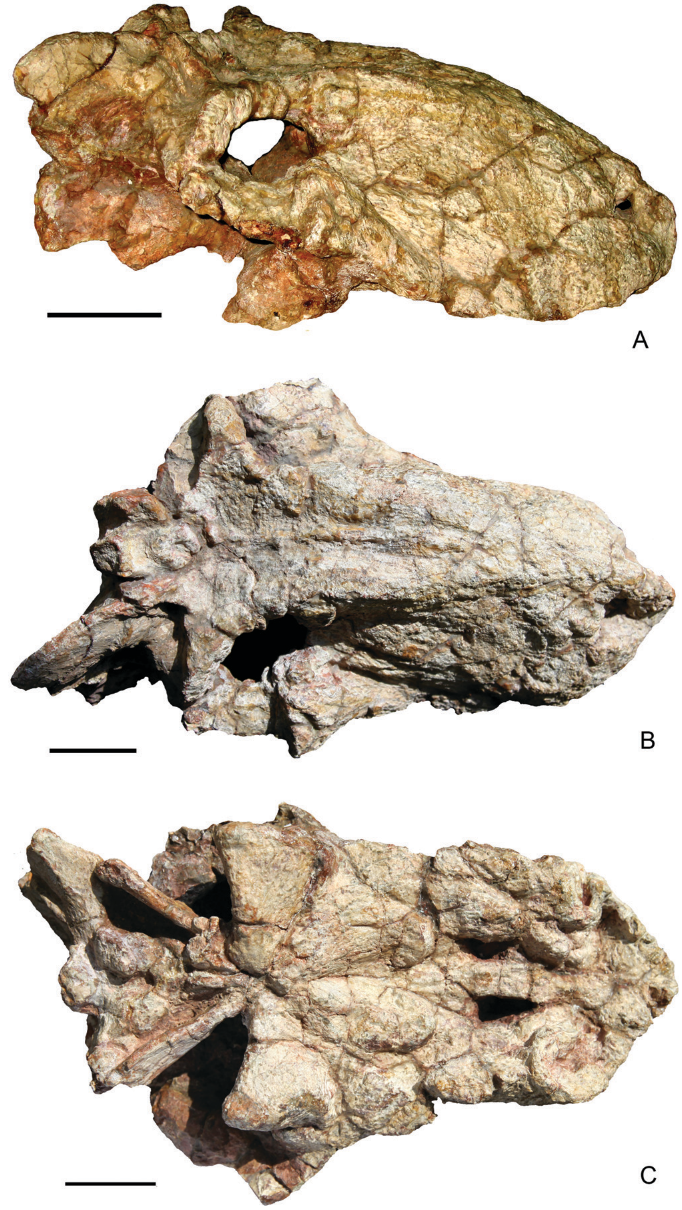

FIGURE 1. *Sinophoneus yumenensis*. Holotype (GMV1601) in **A**, right lateral; **B**, dorsal; and **C**, palatal views. All scale bars equal 10 cm. (Color figure available online.)

The occipital region is nearly vertical, and the occipital condyle cannot be observed in dorsal view. Lateral sides of the occiput flare laterally and slightly posteriorly, so that the occipital plate is slightly concave posteriorly. The occiput is roughly rectangular in shape.

Skull

Premaxilla—The premaxilla forms the anterior tip of the snout, and the anterior and ventral borders of the external naris (Figs. 1–6). Internally, this bone forms a continuous shelf extending from one nostril to the other. The ventral edge of the premaxilla slopes posteroventrally in lateral view. Posteriorly, the

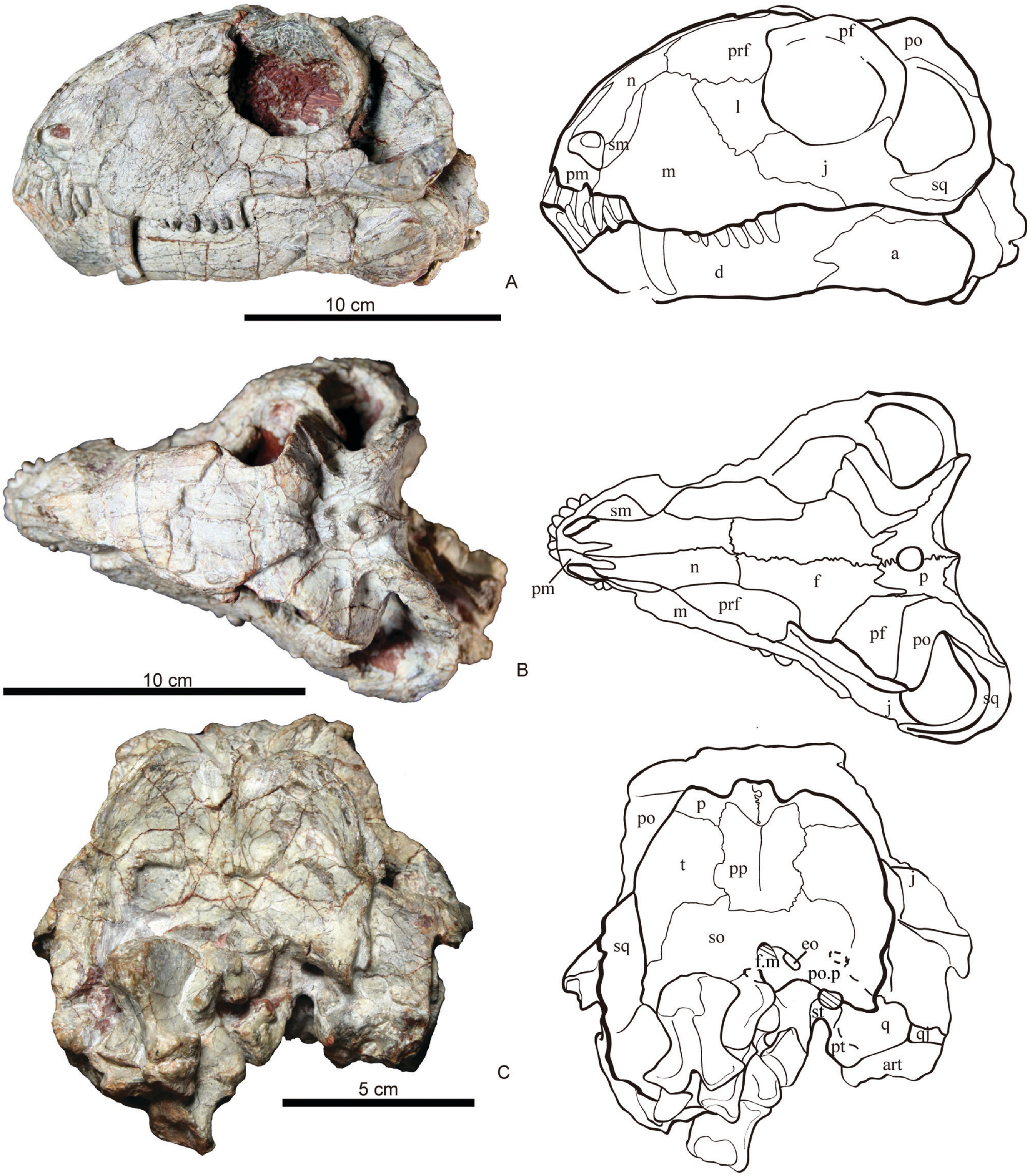

FIGURE 2. *Sinophoneus yumenensis*. Skull with lower jaws (IVPP V18120) in **A**, left lateral; **B**, dorsal; and **C**, occipital views. (Color figure available online.)

TABLE 1. Some measurements of the specimens of *Sinophoneus yumenensis*.

Specimen number	Ls	Lds	Hs	Hoc	Lpc	Lpo	Wtp	Wit	Wp	Dn1	Dn2	Lo	Ho	Lt	Ht
GMV 1601	315	287	~90	>88	62	200	143	72	54	19	17	46	>37	~77	
IVPP V18117	113	114	47	48	26	62	32	32	23	15	10	37	36	25	27
IVPP V18118	~170	146	64	~60	33	85	~56	44	30	18	11	~44	~41	~39	>34
IVPP V18119	179	160	~70	74	41	95	54	57	35	18	15	47	40	40	
IVPP V11820	141	139	69	~69	38	80	62	49	33	16	12	43	41	36	44
IVPP V18121	125	122	~50	49	29	65		>28				36	38	22	29
IVPP V18122	~120	110	45		26	61	~30	28	25	14	8	35	34	23	26
IVPP V18123	~162	140	67	~64	>30		~50	43	21			~44	~40	34–44	32–44
IGCAS V361	120	106	45	52	27	60	31			15	13	40	32		

Abbreviations: **Dn1**, long diameter of naris; **Dn2**, short diameter of naris; **Ho**, orbit height; **Hoc**, occipital height; **Hs**, skull height at anterior margin of orbit; **Ht**, height of temporal fenestra; **Lds**, dorsal skull length, from tip of snot to posterior margin of parietal fenestra; **Lo**, orbit length; **Lpc**: precanine length; **Lpo**, preorbit length; **Ls**, skull length, from tip of snot to occipital condyle; **Lt**, length of temporal fenestra; **Wit**, intertemporal fenestra width; **Wp**, parietal table width; **Wtp**, width of transverse processes of pterygoid.

premaxilla is covered laterally by the maxilla, and the former bone supports the base of the septomaxilla dorsally. The main body of the premaxilla meets its counterpart medially, and contacts the vomers posteriorly. The premaxilla bears a long dorsal process, which becomes more slender as it passes posterodorsally to form a wedge-shaped contact with the nasals. The wedge-shaped contact is also observed in PIN 157/2 (holotype of *Syodon efremovi*) and PIN 157/3 (holotype of *Doliosaurus yanshinovi*), but their nasal anteromedial processes are short (Orlov, 1958). The dorsal process of the premaxilla extends far beyond the level of the posterior border of the external naris.

Five incisor teeth are present in each premaxilla. The incisors are curved and talon-shaped in labial view, and bear distinct heels on their lingual surfaces. Based on well-preserved specimens (Fig. 5), the premaxillary teeth appear to diminish in crown height posteriorly, the first incisor being the largest and the fifth the smallest. The larger incisors measure more than 20 mm in crown height. The first incisor is strongly procumbent, but the degree of procumbency decreases posteriorly so that the fifth incisor is nearly vertical. Medially, a recess between the last upper incisor and the upper canine accommodates the tip of the lower canine. A distinct diastema lies between the incisors and the canine as in *Australosyodon* (Rubidge, 1994), but in contrast to the condition seen in *Syodon* and *Titanophoneus* (Orlov, 1958).

Septomaxilla—The septomaxilla is a slender bone on the lateral surface of the skull (Figs. 2–4). It forms part of the floor of the external naris, as well as the ventral portion of the posterior border of this structure. The posterodorsal process of the septomaxilla is wedged between the maxilla and the nasal, and extends further posteriorly on the snout than does the dorsal process of the premaxilla. The suture between the septomaxilla and the nasal is unclear in most specimens.

Maxilla—The maxilla is large, and nearly triangular in lateral view (Figs. 1–6). Anteroventrally, the maxilla overlaps the lateral surface of the premaxilla to the level of the fourth incisor, so that the fourth and fifth incisors appear to protrude from the maxilla in lateral view. Anteriorly, the maxilla is excluded from the external naris by the septomaxilla. Dorsally, the maxilla contacts the nasal and the anterolateral corner of the prefrontal. Posterodorsally, the maxilla meets the lacrimal along a relatively straight border. Posteriorly, the maxilla abuts the jugal, and the sharp posterior process of the former bone extends along the ventrolateral side of the zygomatic arch to a level posterior to the midpoint of the orbit. The apex of the maxilla lies between the prefrontal and the lacrimal. The lateral surface of the maxilla bears radial striations that converge on the area slightly posterior to the root of the canine. The palatal surface of the maxilla forms the anterolateral border of the internal naris.

The maxilla is generally a thin sheet, apart from a strengthened ventral portion that accommodates the teeth. The inner surface bears a large, round tubercle that contains the root of the upper canine, a large tooth with an elliptical cross-section and serrated mesial and distal carinae. The proximal part of the upper canine is almost vertical, but this tooth becomes slightly curved posteriorly closer to the tip. When the lower jaws are placed in articulation with the skull, the tip of the upper canine lies close to the ventral border of the lower jaw. A diastema is present between the canine and the mesial-most postcanine in specimens other than IVPP V18123, but the existence of the diastema may simply reflect temporary loss of the anterior-most postcanine. Although some maxillae bear only five postcanines, the number varies between six and eight in well-preserved examples, e.g., IGCAS V361, and the middle postcanines are usually larger than the anterior and posterior ones. The postcanines are laterally compressed and spear-shaped, with slightly recurved tips. Their labial surfaces are slightly convex, and their lingual surfaces slightly concave. The postcanines bear serrated mesial and distal carinae.

Nasal—The paired nasals occupy almost the entire roof of the preorbital region (Figs. 1–4), and meet one another along a straight suture. Anteromedially, they bear relatively long processes that extend around the level of the posterior margin of the external nares and separate the dorsal processes of the premaxillae. Anterolaterally, the nasal constitutes the dorsal border of the external naris and contributes slightly to internarial bar. Laterally and ventrally, it forms a long sutural contact with the septomaxilla and the maxilla. Posterolaterally, the nasal sutures with the prefrontal. Posteriorly, the nasal forms a transverse sutural contact with the frontal slightly anterior to the level of the anterior rim of the orbit.

Lacrimal—The lacrimal is a relatively large quadrangular element that contributes to the anterior border of the orbit (Figs. 1–4, 6). It extends forward ventral to the prefrontal, but terminates slightly posterior to the level of the anterior end of the prefrontal. The lacrimal meets the maxilla anteroventrally, and the jugal posteroventrally. The lateral surface of the lacrimal is smooth and nearly flat.

Prefrontal—The elongate prefrontal occupies the transition between the dorsal and lateral surfaces of the skull, making the outer surface of this bone convex (Figs. 1–4, 6). Anteroventrally, the prefrontal forms a short suture with the maxilla. Medially, the prefrontal has a convex border that contacts the nasal anteriorly and the frontal posteriorly. The prefrontal forms the anterodorsal border of the orbit.

Frontal—The frontal forms a large part of the interorbital region (Figs. 1–4), and has a laterally tapering process that forms a small portion of the dorsal border of the orbit between the

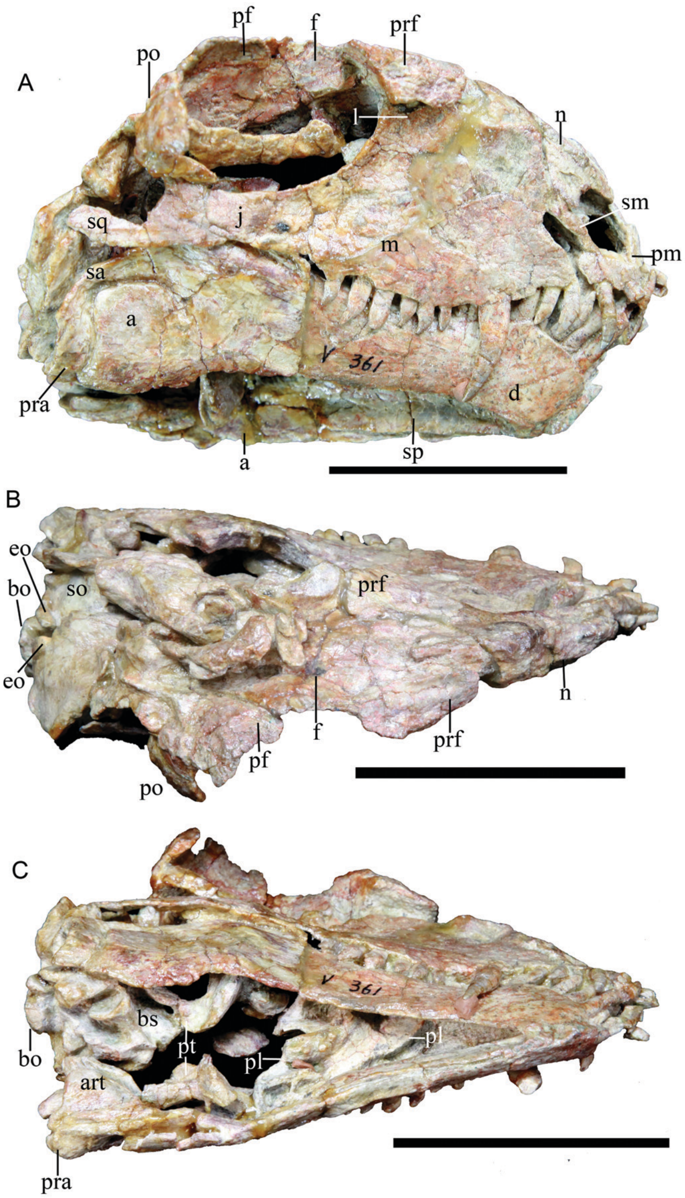

FIGURE 3. *Sinophoneus yumenensis*. IGCAGS V361 (holotype of *Stenocybus acidentatus*) in **A**, right lateral; **B**, dorsal; and **C**, palatal views. Scale bars equal 5 cm. (Color figure available online.)

prefrontal and the postfrontal. The frontal is an elongate bone that has sutural contacts with the nasal anteriorly and the parietal posteriorly, and meets its counterpart in the midline along a straight suture. The posterolateral process of the frontal extends posteriorly to the level of the anterior margin of the pineal foramen. The posterior margin is relatively wide and has a zigzag appearance, a condition similar to that seen in *Archaeosyodon* (pers. observ.).

The midline between the two frontals is raised as a low ridge, which forms a boss at the level of the anterior margin of the postfrontal. This boss is indistinct in the holotype but clearly developed in IVPP V18117 and V18120. Lateral to the ridge, the dorsal surface of the frontal is slightly concave. The posterolateral process of the frontal bears a deep fossa medial to the postfrontal.

The frontal slopes ventromedially to form a ventral crista, which extends anteriorly to a point ventral to the posterior process of the prefrontal. The crista extends anterolaterally. The ventral surface of the paired frontals forms a trough between the ventral cristae in IVPP V18119. The trough is hourglass-shaped in ventral view, with a smooth inner surface, and probably represents the passage for the olfactory tract.

Postfrontal—The thickened postfrontal expands slightly laterally, and forms the posterodorsal border of the orbit (Figs. 1–4, 6). Its suture with the postorbital extends medially from this part of the orbital margin. Approaching the pineal foramen, the suture turns posteriorly and terminates near the posterior border of the skull roof, and a robust ridge rises on this suture. The medial sutural border of the postfrontal is curved, meeting the frontal anteriorly and the parietal posteriorly. The postfrontal has a long and pointed posterior process that inserts between the parietal and the postorbital, and extends far posterior to the anterior margin of the parietal. The postfrontal barely extends posterior to the anterior margin of the parietal in most anteosaurids other than *Archaeosyodon* (Orlov, 1958; Rubidge, 1994; Ivakhnenko, 2003).

Parietal—The parietal is narrow anteriorly but wide posteriorly, and bears a well-defined chimney around the pineal foramen in the skull midline (Figs. 1–4). The anterior border of the chimney approaches the frontal, whereas the posterior border of the chimney lies on the posterior border of the skull roof. Anterior and anterolateral to the pineal foramen, the parietal forms an interdigitated contact with the frontal. The parietal meets the postfrontal laterally, has a long sutural contact with the postorbital posterolaterally, and meets the tabular posteriorly and the postparietal posteromedially. Anterior to the pineal foramen, the parietal meets its counterpart along a tightly meandering suture. Behind the pineal foramen, the suture between the two parietals is short and vertical. The posterior region of the parietal contributes extensively to the dorsal portion of the occipital plate.

Postorbital—The postorbital is a strongly curved bone that forms the entire posterior border of the orbit, as well as the dorsal border of the temporal fenestra (Figs. 1–4, 6). Posteroventrally, it has a long sutural contact with the jugal extending down to the ventral margin of the orbit, and forms the postorbital bar together with the jugal. The postorbital bar is anteroposteriorly thin but mediolaterally wide, and narrows ventrally so that its outline in posterior view is roughly triangular. The postorbital contacts the postfrontal anteriorly and medially, and contacts the parietal posteromedially. The dorsal surface of the postorbital is strongly recessed, and gives origin to part of the adductor musculature. The postorbital does not contribute to the intertemporal part of the skull roof, which is narrower than the interorbital region. The posterior process of the postorbital extends along the edge of the temporal fenestra, and is in contact with the squamosal ventrally and the tabular posteriorly.

Jugal—The jugal is a large, triradiate bone with a flat lateral surface (Figs. 1–4, 6). A long anterior (suborbital) process forms the ventral margin of the orbit, meeting the ventral process of the lacrimal. The anterior end of this process, which has a concave lateral surface, extends forward beyond the level of the anterior margin of the orbit. The anterior process is of nearly constant height along its length. The pointed dorsal process of the jugal contributes to the postorbital arch, forming part of the anterior margin of the temporal fenestra. The posterior process tapers slightly in the posterior direction and ultimately meets the squamosal and the quadratojugal, forming the ventral border of the temporal fenestra.

Squamosal—The squamosal forms the posterior border of the temporal fenestra, and overlaps the lateral surface of the jugal to contribute to the ventral margin of this opening (Figs. 2–4, 6). The squamosal extends anteriorly for more than two-thirds of the

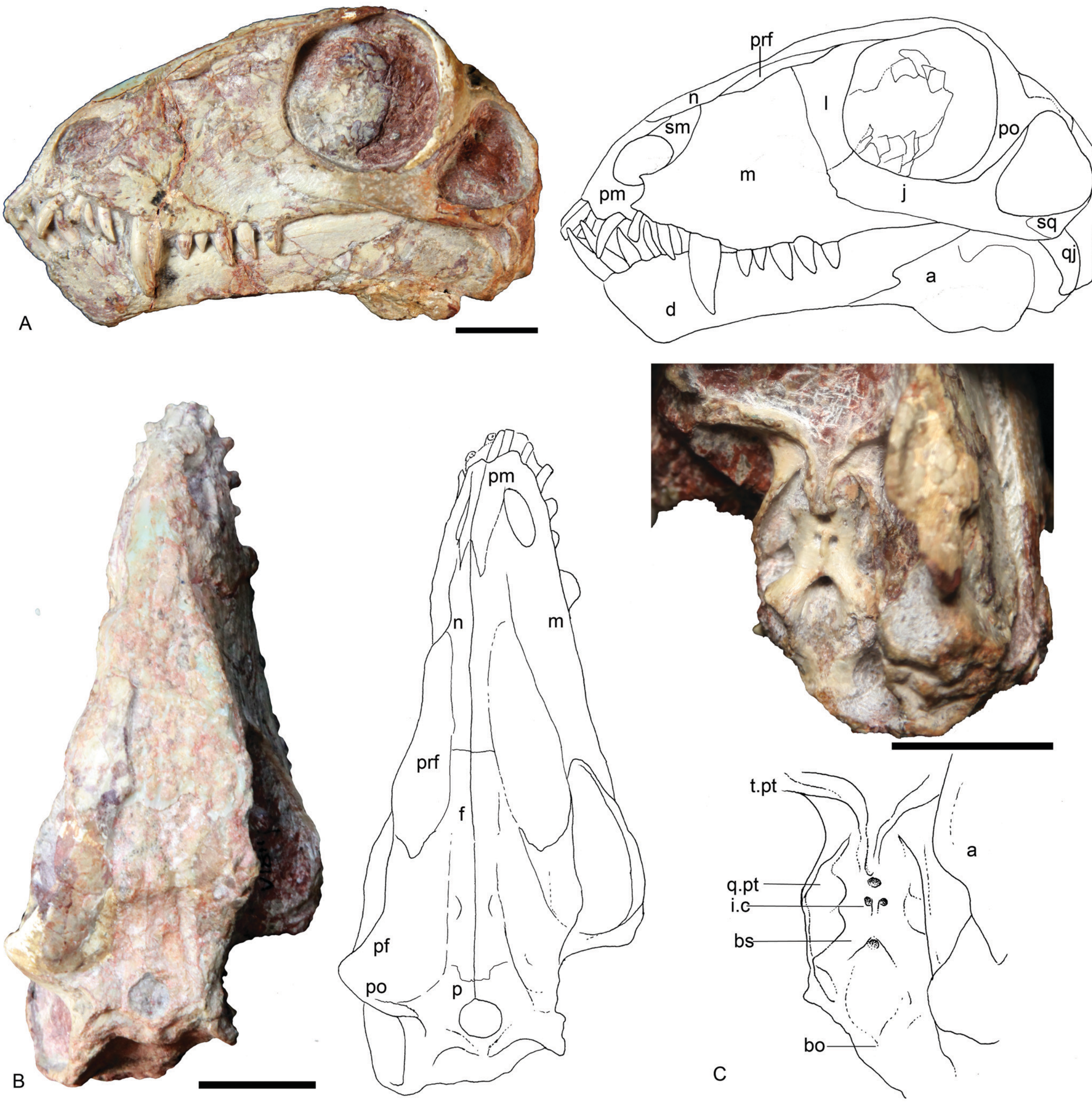

FIGURE 4. *Sinophoneus yumenensis*. IVPP V18117 in **A**, right lateral; **B**, palatal; and **C**, dorsal views. Scale bars equal 2 cm. (Color figure available online.)

length of the lower temporal bar, but stops short of the anterior margin of the fenestra. The squamosal extends medially to form a plate-like body, which meets the bones of the occiput along a ridge on its posterior side. The squamosal contacts the postorbital dorsally and the tabular posterodorsally. Ventrally, the lateral side of the squamosal contacts the quadratojugal, whereas the medial side contacts the quadrate (Figs. 2, 7).

The squamosal forms the posterior border of the temporal fenestra and it is from the margins of this bone that much of the adductor musculature originates, and is exposed in dorsal view. This bone is narrowly exposed in occipital view. A distinct groove, representing the external auditory meatus, is situated lateral to the suture between the squamosal and the tabular. A pointed ventral process of the squamosal passes posterior to the quadrate and

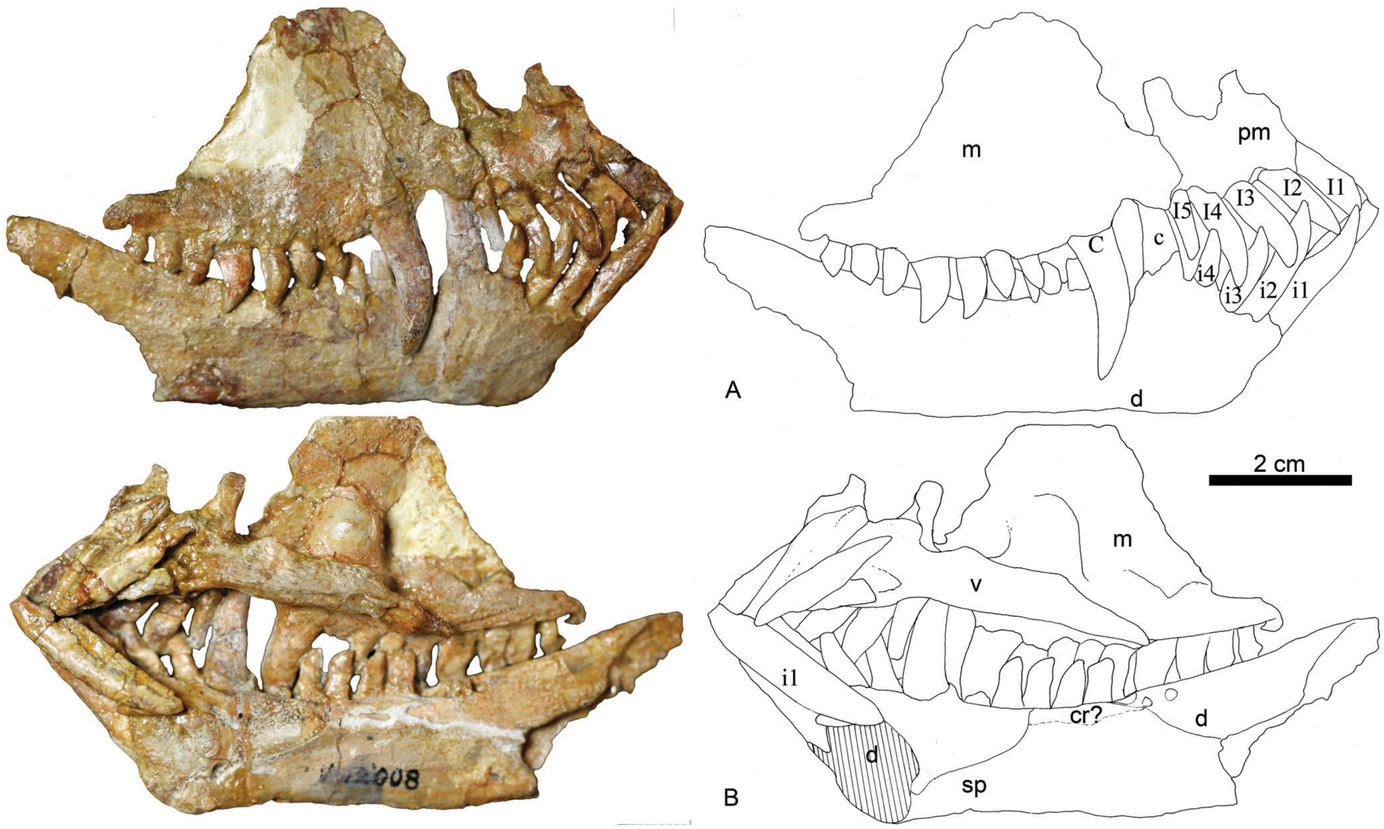

FIGURE 5. *Sinophoneus yumenensis*. IVPP V12008 in **A**, lateral and **B**, medial views. (Color figure available online.)

quadratojugal, and descends beyond the level of the ventral edge of the paroccipital process.

Quadratojugal—The narrow quadratojugal lies on the lateral side of the quadrate (Figs. 2, 6, 7), and the ventral contact between the two bones is situated immediately above the lateral articular condyle of the latter. The quadratojugal has an expanded footplate that extends medially beyond the edge of the quadratojugal foramen and overlaps the posterodorsal side of the lateral articular condyle of the quadrate. Lateral to the foramen, the quadratojugal is relatively narrow in occipital view, but dorsal to the foramen the quadratojugal flares anteriorly and laterally to contact the posterior process of the jugal. The quadratojugal is sutured with the lateral side of the dorsal expansion of the quadrate and bears a deep fossa on their anterior surface. The quadratojugal does not extend as far dorsally as the quadrate.

Postparietal—The postparietal (interparietal) is an unpaired midline element located near the dorsal edge of the occiput (Figs. 2, 7). It forms an 'M'-shaped suture with the parietal dorsally, an irregular sutural contact with the tabular laterally, and a nearly horizontal contact with the supraoccipital ventrally. The maximum width of the postparietal is roughly equal to its height. The posterior surface of the postparietal bears a keel-like median ridge.

Tabular—The tabular is a narrow, high, irregularly shaped bone that tapers ventrally and extends well below the level of the posttemporal fenestra (Figs 2, 7). It is in contact with the parietal dorsally, the postorbital dorsolaterally, the squamosal laterally, the postparietal medially, and the supraoccipital ventromedially. The ventral tip of the tabular contacts the paroccipital process of the opisthotic, but is excluded from the lateral margin of the posttemporal fenestra by the supraoccipital.

Vomer—This bone is hardly visible in most specimens because the mandible is preserved in tight articulation with the skull, but it is well exposed in the holotype (Fig. 1). The paired vomers are narrow, vertically expanded bones (Figs. 1, 5), and the midline suture between them is hardly recognizable in large specimens. The vomer extends anteriorly to the level of the fourth incisor, and underlies the premaxilla as in other dinocephalians. The vomer is elongate and edentulous, and forms the medial and posteromedial borders of the choana. The ventral surface is nearly flat, although the anterior portion of this surface is slightly convex. No ventrally protruding ridge as in other anteosaurs is observed on the lateral side of the exposed vomer in IVPP V18119. The wide postchoanal portion of the vomer contacts the palatine laterally, and tapers toward the midline as it passes posteriorly from the level of the palatine bosses to a possible contact with the pterygoid. This contact would be situated at the level of the fourth postcanine in IVPP V12008. The vomer meets the maxilla medial to the canine, and this contact lies at the anterior end of the choana in the holotype.

Palatine—The right palatine is well exposed in IVPP V18123 (Fig. 7). An anteriorly directed process of the palatine extends along the medial side of the maxilla, continuing anteriorly to the level of the second postcanine, and forms the posterolateral border of the choana. Posteromedially, the palatine forms a prominent, anteriorly rounded, ventrally projecting boss together with the pterygoid. The anterior and anterolateral margins of this boss are studded with small conical teeth. Teeth are also present on the medial side of the boss in IVPP V18118. Only one tooth row is

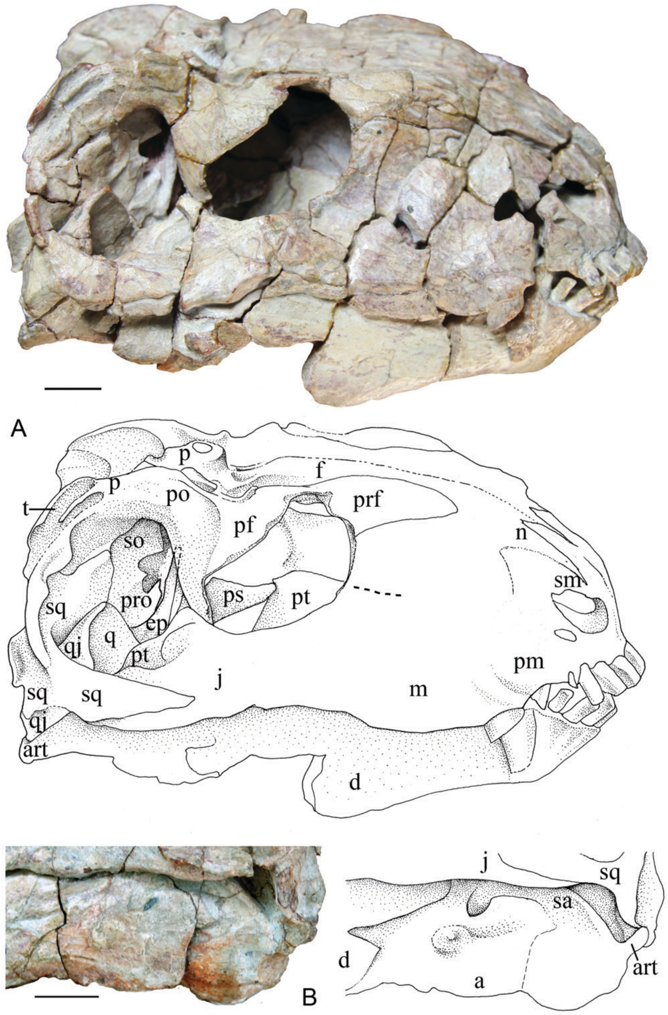

FIGURE 6. *Sinophoneus yumenensis*. IVPP V18119 in **A**, right and **B**, left lateral views. Scale bars equal 2 cm. (Color figure available online.)

present in IGCAS V361 (Fig. 2) and IVPP V18118, but two rows are present in IVPP V18123 (Fig. 7). The root of a large palatine tooth is situated lateral to the boss and medial to the suture with the ectopterygoid in IVPP V18118 and V18120.

Ectopterygoid—The edentulous ectopterygoid is a relatively large, triangular bone, and is well preserved on the right side of the skull in IVPP V18119 and V18123 (Fig. 7). This bone covers much of the anterior face of the transverse flange of the pterygoid and is in contact with the pterygoid posteriorly, the palatine anteromedially, and the maxilla dorsolaterally. The ectopterygoid is strongly curved, giving a vaulted topology on the palate.

Pterygoid—The pterygoid is a complex bone with anterior, lateral, quadrate, and dorsal rami (Figs. 1, 3, 4, 6, 7). It accounts for more than half the length of the palate. The anterior ramus of the pterygoid contributes to the palatal boss, and is contact with the palatine anterolaterally. The pterygoid portion of the palatal boss is ventrally convex and slightly less prominent than the palatine boss, and meets its own counterpart in the midline. A cluster of small denticles studs the posterior region of the pterygoid boss, and this cluster is continuous across the midline. The lateral ramus of the pterygoid extends transversely across the palate, and is inclined only slightly ventrally. The ventral surface of the lateral ramus is ridge-like, and is confluent with the ventral surface of the basicranial ramus of the pterygoid. The ventral margin of the transverse flange bears a single row of teeth in some specimens (IVPP V18117, V18120), but two rows of teeth are clearly evident in IVPP V18123. The ventral surface of the basicranial ramus of the pterygoid bears a sharp parasagittal ridge. A trough is present between the left and right basicranial rami, although an interpterygoid vacuity is absent. Immediately posterior to the basicranial ramus, the pterygoid meets the basisphenoid.

The pterygoid forms a subhorizontal shelf between the basicranial and quadrate rami. The posterior margin of this shelf contacts the basipterygoid process of the basisphenoid, and all together form the anterior border of the cranioquadrate passage. The basipterygoid articulation lies just dorsal to the basicranial ramus of the pterygoid. The vertically deep quadrate ramus of the pterygoid extends posterolaterally to meet the medial surface of the quadrate, extending as far as the posterior edge of the latter bone. The dorsal ramus is visible through the orbit in IVPP V18119. The pterygoids form a high, prominent midline septum, which is triangular in lateral view. Posteriorly, the pterygoids clasp the anterior end of the median septum formed by the parasphenoid. The anterior extent of the pterygoid is uncertain due to coverage by the maxilla.

Quadrate—All known quadrates of *Sinophoneus yumenensis* are preserved in articulation. The quadrate is a relatively large and robust element with a fan-like shape (Figs. 2, 6, 7). The dorsal process of the quadrate extends above the level of the lower temporal bar and is visible in lateral view. In dorsal view, the quadrate appears to bear an anterior process extending from the medial margin of its dorsal apex. This process represents the dorsal margin of an extensive quadrate flange, the anterior surface of which is concave.

The quadrate contacts the quadratojugal laterally, and both bones appear to emerge from below the squamosal and the paroccipital process in posterior view. Medially, the quadrate is in contact with the anterior side of the paroccipital process of the opisthotic and with the stapes, and also forms a triangular contact with the posterolateral surface of the quadrate ramus of the pterygoid. The articular surface of the quadrate is inclined anteromedially and bears two convex, anteroposteriorly narrow condyles that are separated by an obliquely oriented trough. The medial condyle is wider than the lateral one.

Supraoccipital—The supraoccipital is a transversely broad bone that appears completely fused to the opisthotic in posterior view (Figs. 2, 7). It forms the dorsal margins of the foramen magnum and posttemporal fenestra. Immediately above the foramen magnum, the supraoccipital swells to form a broad median ridge. The posttemporal fenestra is a small, elliptical opening whose long axis is nearly horizontal. The supraoccipital forms a short suture with the postparietal dorsomedially, but its lateral and dorsolateral edges form long sutural contacts with the tabular in occipital view. It is also in contact with the tabular laterally in the anterior surface of the occiput.

The dorsal part of the supraoccipital sends a flange anteriorly to form the dorsal part of the side wall of the braincase (Fig. 6). Another process of the supraoccipital descends ventrally to meet the ascending process of the prootic. The groove for the blood vessels extending forward from the posttemporal fenestra lies above the trigeminal foramen.

Exoccipital—In many specimens the exoccipitals and basioccipital are covered by anterior cervicals, but they are well exposed in IGCAS V361 and IVPP V18119. Small, paired exoccipitals protrude posteriorly from the lateral margins of the foramen magnum (Figs. 2, 3). As in *Titanophoneus*, the exoccipitals fail to contact one another above the foramen magnum, but are in contact on the

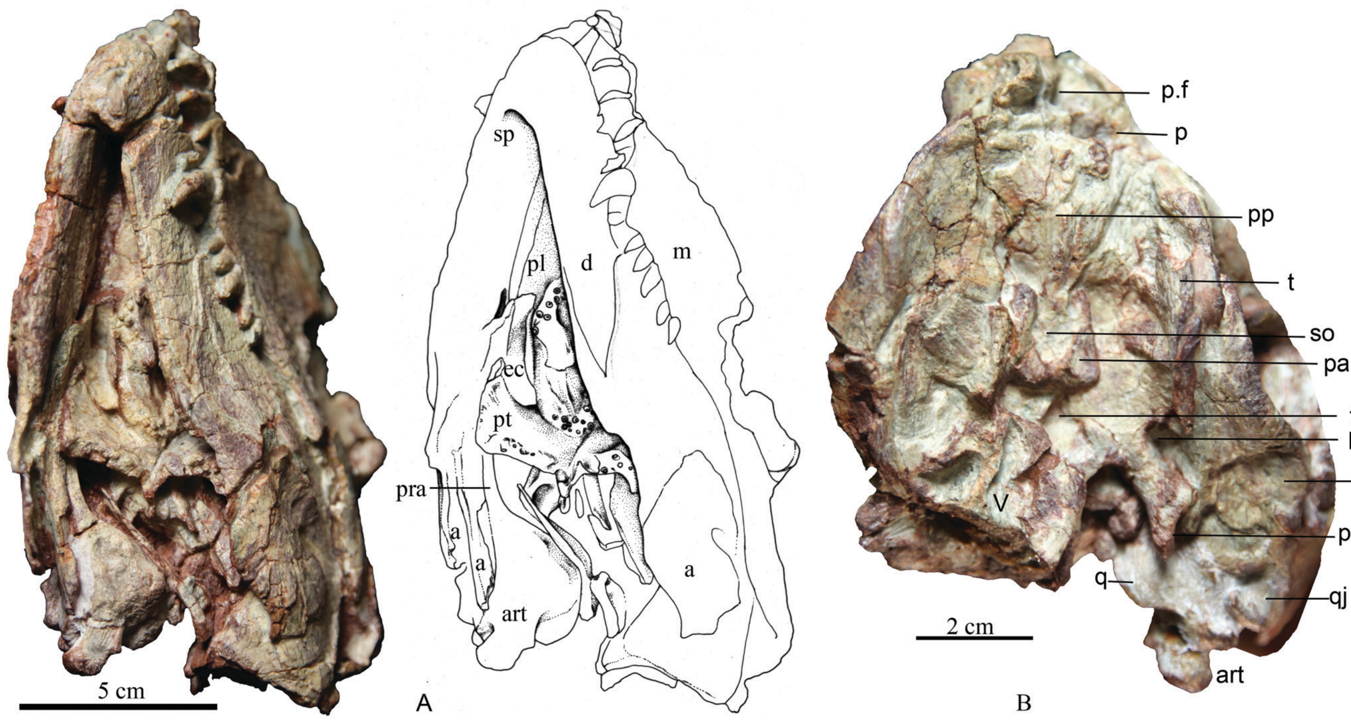

FIGURE 7. *Sinophoneus yumenensis*. IVPP V18123 in **A**, ventral and **B**, occipital views. (Color figure available online.)

dorsal surface of the occipital condyle (Orlov, 1958). Below the lateral process of the exoccipital, a large jugular foramen is positioned between the exoccipital and opisthotic.

Basioccipital—The basioccipital forms only the ventral portion of the occipital condyle, which is large and somewhat trifurcate (Figs. 1, 3, 4). The basioccipital meets the basisphenoid anteroventrally, and the opisthotic ventrolaterally and laterally.

Prootic—The prootic is ankylosed to the anterior faces of the opisthotic and supraoccipital, and has only a small lateral surface (Fig. 6). An ascending process meets the supraoccipital, and the anterior part of this process bears a trigeminal notch. Ventrally, the prootic rests on the ascending part of the basisphenoid to form the anterolateral edge of the dorsum sellae.

Opisthotic—The opisthotic has a gently convex posterior surface and deepens toward its lateral end, where it is overlapped by the tabular (Figs 2, 3, 7). The paroccipital process is a massive bar, divided by a distinct edge into posterior and ventral faces. Medially, it meets the exoccipital, basioccipital, and basisphenoid. The ventral face of the opisthotic expands in the direction of its lateral end, which contacts the quadrate and forms the posterior border of the cranioquadrate passage.

Basisphenoid—The basisphenoid is a relatively small bone whose anterior portion bears a ventral midline keel flanked by the carotid foramina (Figs. 1, 4). The anterolateral corners of the basisphenoid extend dorsally and laterally to form basipterygoid processes that suture to the medial sides of the quadrate rami of the pterygoids. The sutural line of the basicranial joint is clear in small specimens but invisible in large ones. Posteriorly, paired posterolateral rami of the basisphenoid form a fossa between them. Each posterolateral ramus is in contact with the basioccipital and opisthotic dorsolaterally, and forms the anterior and ventral margins of the fenestra ovalis.

Parasphenoid—The parasphenoid forms a median septum that is roughly triangular in lateral view (Fig. 6). The anterior end of the septum is pointed, and meets the pterygoid as in *Dimetrodon* (Romer and Price, 1940:pl. 7). In *Anteosaurus* and *Jonkeria*, the anterior end is pointed, but does not touch the pterygoid; in *Struthiocephalus*, the anterior end meets the pterygoid but is wide (Boonstra, 1968:figs. 5, 31, 45). A distinct presphenoid cannot be identified. No orbitosphenoid is apparent. In most specimens, the parasphenoid is not visible in ventral view, but this bone appears to be fused ventrally to the basisphenoid in IVPP V18117 (Fig. 4).

Epipterygoid—The epipterygoid lies lateral to the braincase, and covers the anterior portion of the open lateral sella (Fig. 6). The epipterygoid rests on the quadrate ramus of the pterygoid, and is positioned lateral to the basisphenoid and prootic. The footplate of the epipterygoid is anteroposteriorly expanded, with a distinct posterior process as in *Dimetrodon* and *Anteosaurus*. The epipterygoid extends dorsally and slightly anteriorly as a mediolaterally flattened pillar of bone with a fairly straight anterior margin and a concave posterior one. The upper part of the epipterygoid forms a flat dorsal margin, which does not reach the parietal. In *Dimetrodon* and *Anteosaurus*, this bone nearly reaches the skull roof (Romer and Price, 1940; Boonstra, 1968).

Stapes—A right stapes is preserved in situ in IVPP V18120 (Fig. 2C), and a left stapes can be identified in IVPP V18117. This short, massive bone fits into a pit on the inner surface of the quadrate. The stapes extends medially from the posterior part of the medial surface of the quadrate, immediately behind the quadrate ramus of the pterygoid, to the fenestra ovalis. This fenestra is bounded by the prootic, opisthotic, and basisphenoid. In ventral view, the distal end of the stapes appears to be expanded anteroposteriorly where it meets the quadrate. However, the stapes tapers towards the medial footplate that contacts the fenestra

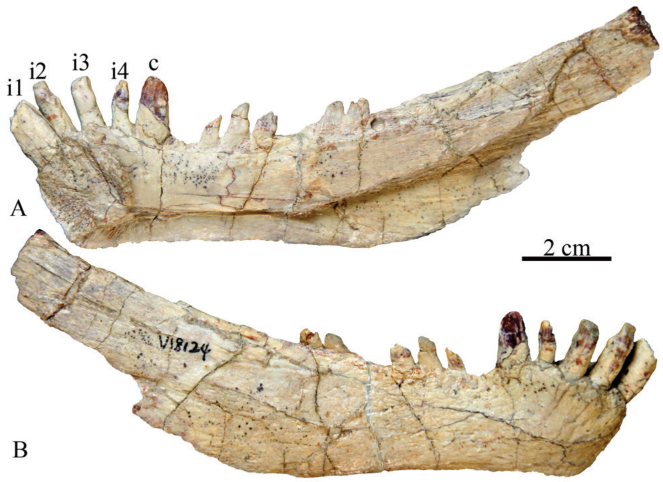

FIGURE 8. Dentary of *Sinophoneus yumenensis*. IVPP V18124 in **A**, medial and **B**, lateral views. (Color figure available online.)

ovalis. In posterior view, the medial part of the stapes is also narrower than the lateral part. No stapedial foramen is evident.

Scleral Ossicles—Some scleral ossicles are preserved in the left orbit of the IVPP V18117 (Fig. 4A). However, the arrangement of these elements is unclear.

Lower Jaw

Dentary—The dentary is the largest element of the lower jaw, and forms most of the lateral surface of this structure (Figs. 2–8). The lateral surface of the dentary is relatively flat, with some small nutrient foramina. Anterior to the lower canine, the upper margin of the dentary is inclined anteroventrally, corresponding to the tilted lower margin of the snout formed by the premaxilla and maxilla. Immediately posterior to the lower canine, the lateral surface of the dentary forms a vertically indentation to accommodate the upper canine, which passes lateral to the lower jaw when the mouth is closed. This is the dorsoventral thinnest point of the dentary. The posterior part of the upper margin of the dentary extends posterodorsally until it reaches its highest point below the temporal fenestra. The lower margin of the dentary is nearly straight until the level of the last postcanine, then turns upwards.

The dentary forms a very rugose symphysial surface in the anterior midline for contact with its opposite counterpart. A long slot extends from the symphysial area to the posterodorsal end of the dentary, along the ventral edge of the medial surface of the dentary (Fig. 8). This slot carries the splenial medially, the angular and the prearticular posteriorly, and the surangular posterodorsally. In lateral view, the middle part of the posterior margin of the dentary is incised, as in *Syodon*.

The dentary bears four incisors, a single canine, and approximately six to nine postcanines. The lower incisors intermesh with the upper incisors when the jaws are closed, and the first pair of upper incisors lies between the first pair of lower incisors. As in *Titanophoneus*, the first incisor is the largest, the fourth is the smallest, and the second and third are similar to one another in size. The incisors each have a small heel on the lingual surface, and the talon distal to this heel constitutes roughly half of the length of the tooth crown. The inner surface of the crown faces slightly distally, as well as lingually. The incisors are compressed mesiodistally to varying degrees, whereas the first incisor is nearly flat in this direction. The lower canine resembles the upper one in lacking serrations along the carinae and is smaller than the upper one. The lower postcanines are similar in shape to the upper postcanines. The lower postcanine row does not extend as far posteriorly as the upper one.

Splenial—The splenial is a flat bone on the medial side of the lower jaw that makes a small ventral contribution to the symphysis (Figs. 5, 7). The dorsal margin slopes upwards as far posteriorly as the third postcanine, then remains approximately horizontal until the level of the seventh postcanine. At this point, the dorsal margin of the splenial begins to slope downwards as it extends posteriorly towards the angular and prearticular.

Coronoid—A small piece of element lying above the splenial and medial to the postcanine root is identified as the coronoid (Fig. 5).

Angular—The angular is a large posteroventral element that forms a large part of the lateral surface of the lower jaw (Figs. 2, 3, 4, 6, 7), lying behind the splenial, below and behind the dentary, and below the surangular. The angular is exposed medially below the prearticular, and contributes to the border of the Meckelian fossa.

The reflected lamina is exceptionally large. The lower margin of the lamina protrudes below the lower margin of the main shaft of the jaw, but the posterior margin of the lamina is distinctly anterior to that of the lower jaw. The dorsal notch lies above the middle part of the reflected lamina. The anteroposterior distance between the dorsal notch and the dentary is short, and subequal to the anteroposterior distance to the articular. In ventral view, the angular can be seen to fit between the dentary and splenial.

A boss is visible near the anterior border of the lateral surface of the left angular of IVPP V18119 (Fig. 6B). No similar boss is evident in other individuals, so this is probably an abnormal feature restricted to one atypical specimen rather than evidence that an angular boss is present in *Sinophoneus*. The anterodorsal corner of the bone bulges laterally in IVPP V18120, but does not form a boss. No distinct boss is discernible in other known specimens.

Surangular—The surangular forms the posterodorsal part of the lower jaw (Figs. 2–4), but has only a small lateral exposure. The surangular extends anteriorly and forks into two processes: a dorsal one forming the apex of the lower jaw above the dentary, and a ventral one exposed between the dentary and the angular and anterior to the dorsal notch of the angular. The surangular thickens to form a moderately prominent shelf that overhangs its smooth, slightly concave lateral surface.

Prearticular—The prearticular is a thin, strap-shaped bone (Fig. 7A). Anteriorly, the prearticular contacts the dentary laterally, the splenial ventrally, and the tentatively identified coronoid fragment dorsally. The prearticular extends posteriorly to the articular, flanked by the surangular above and the angular below, but the suture between the prearticular and the articular is unclear. Close to the articular, the prearticular twists about its long axis to achieve a more horizontal orientation, and widens transversely in ventral view to match the width of the articular.

Articular—All known examples of the articular are preserved in articulation with the quadrate, so that the dorsal side of the articular is hardly visible (Figs. 2–4, 6, 7). The articular sutures with the angular laterally, and the prearticular anteroventrally. The glenoid region of the articular consists of two concave, transversely oriented facets. IVPP V18123 shows that a retroarticular process is present on the lateral side of the articular (Fig. 7A).

Postcranial Axial Skeleton

Numerous therapsid postcranial elements are known from the Dashankou locality, but only a few can be reliably referred to *Sinophoneus yumenensis*. The following description is mainly based on IVPP V18120 and V18127. IVPP V18120 includes 12

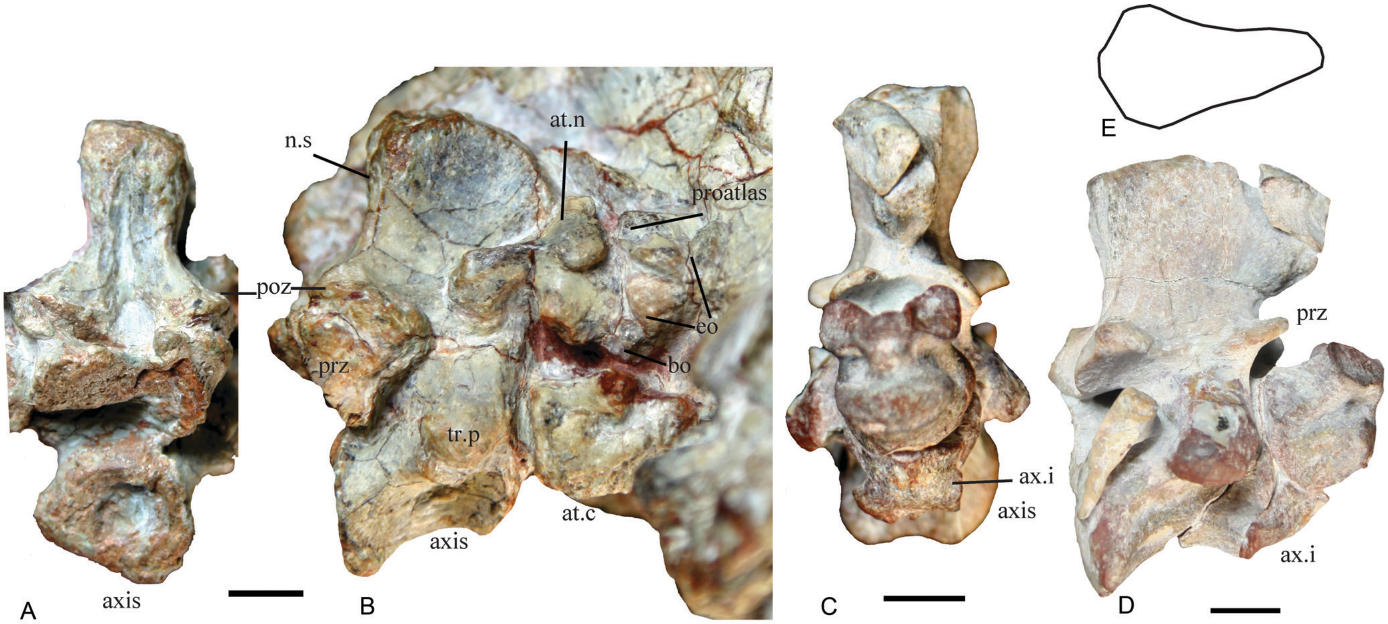

FIGURE 9. Atlas-axis complex of *Sinophoneus yumenensis*. IVPP V18120 in **A**, posterior and **B**, right lateral views; IVPP V18127 in **C**, anterior; **D**, right lateral; and **E**, dorsal views. Scale bars equal 1 cm. (Color figure available online.)

anterior presacral vertebrae preserved with the corresponding ribs, and pectoral girdle elements (Figs. 9, 10).

The proatlas is preserved with the skull in most specimens. In IVPP V18123, the halves of the proatlas attach to the two sides of the mid-occipital ridge, just above the foramen magnum (Fig. 7). In IVPP V18120, the right half proatlas lies above the occipital condyle (Fig. 2C). The proatlas is a flat bone with a nearly triangular shape. Its ventral base is rather broad, articulating anteriorly with a facet on the exoccipital and posteriorly with the atlantal neural arch.

The right half of the atlantal neural arch is exposed in IVPP V18120 and seems to be separate from its counterpart on the left

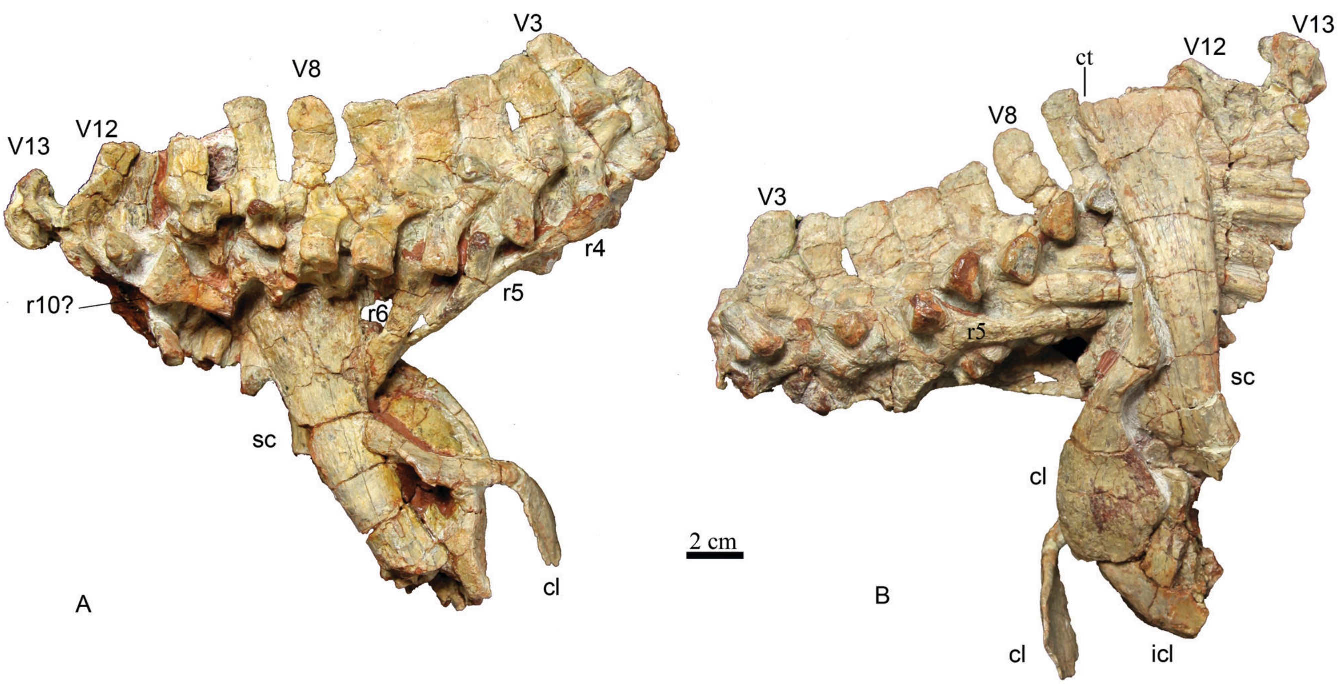

FIGURE 10. Presacral vertebrae and pectoral girdles of *Sinophoneus yumenensis*. IVPP V18120 in **A**, right and **B**, left lateral views. (Color figure available online.)

(Figs. 2, 9). The right portion of the neural arch has a massive, rectangular pedicel, a low neural spine, and a rather long posterior process that articulates ventromedially with the prezygapophysis of the axis. The rib facet is knob-like and positioned on the middle part of the lateral surface.

The atlantal centrum is pentagonal in lateral view, with the horizontal base of the pentagon positioned dorsally and its most acute angle directed anteriorly (Fig. 9). The dorsal surface of the centrum is concave, to accommodate the spinal cord. The ventral part of the centrum is beveled for intercentra both anteriorly and posteriorly, leaving only a short ventral margin. The atlantal centrum is shorter and slightly lower than the following centra. The atlantal intercentrum is preserved in articulation with the atlantal centrum in IVPP V18120, but the suture between these elements is still visible.

The axial neural arch is fused to the centrum along a persistently visible suture, and the neural arch is morphologically almost identical to those of *Titanophoneus* and *Syodon* (Orlov, 1958:fig. 36) (Fig. 9). The axial neural arch is massive, with a longitudinally expanded neural spine that inclines forward and somewhat overhangs the atlas. The neural spine has a rugose dorsal edge, expands laterally backwards, then pinches inwards on posterior end. A vertical middle groove runs between the posterior edges of the spine. The articular surfaces of the zygapophyses are closer to the horizontal than to the vertical. The short transverse process bears an elongated, ventrolaterally directed articular surface for the tuberculum of the axial rib. The short parapophysis is directed dorsolaterally and slightly anteriorly. The axial centrum is subcircular in anterior and posterior views, and the posterior end is wider than the anterior end. The ventral surface of the centrum bears a low, blunt ridge, whereas the lateral surfaces are concave.

The axial intercentrum is papilionaceous in ventral view and wedge-like in lateral view. It does not reach the atlantal intercentrum anteriorly, but extends posteriorly beyond the anterior margin of the axial centrum and forms a small facet for articulation with the capitulum of the axial rib. The angle between the ventral surfaces of the atlantal centrum and intercentrum is about 135° in lateral view.

Posterior to the axis, the centra are strongly concave between the level of the transverse process and the ventral ridge, so that the lower portion of each centrum is rather thin in cross-section. A sharp ventral keel is present on at least the third to seventh centra (Fig. 10). The transverse processes increase posteriorly in both anteroposterior and transverse width until the seventh vertebra. The transverse process of the eighth vertebra is similar to that of the seventh, but those of more posterior vertebrae are distinctly slender and slightly narrower. Due to preservational distortion, the transverse process on the left side of each vertebra in IVPP V18120 is wider and shorter than the corresponding right one. Each prezygapophysis has a ventral base, which merges with the transverse process posteroventrally, and a dorsal margin directed towards the base of the neural spine. The anteroposterior width of the neural spine increases slightly from the third to the seventh vertebra, measuring 14.5 and 17.5 mm in the third and sixth vertebrae, respectively. The spines are distinctly narrower and higher from the eighth vertebra than that those of the third to seventh vertebrae.

Based on the position of the scapula and the morphological changes seen along the vertebral column, the number of cervicals may be eight, but the possibility that the eighth vertebra is a dorsal cannot be excluded.

The ribs are preserved beginning from the third vertebra, but the head is only exposed in the third to sixth ribs and in the 10th. All of the available rib heads are flattened in the plane of the rib. All of the cervical ribs are dichocephalous: the short, wide tuberculum contacts the transverse process, and the long, narrow capitulum contacts the centrum. The free distal end of each rib narrows rapidly and is directed posteroventrally. The more posterior ribs are much longer than the more anterior ones. An anterior dorsal rib, the 10th, is also two-headed, but the tuberculum is only a slight prominence on the rib head.

Pectoral Girdle

The enlarged anterior portion of the interclavicle is preserved (Fig. 10). Near the anterior margin of the bone, the ventral surface bears paired concavities, one of which is preserved in articulation with the left clavicle.

The clavicle is moderately expanded ventrally, but narrow dorsally (Fig. 10). Its posterior edge is grooved, and overlaps the anterior border of the scapula. Several fine, nearly parallel striations are visible on the external surface of the ventral plate and the straight portion of the shaft. A cleithrum is preserved on the anterodorsal corner of the blade of the left scapula (Fig. 10B). It is small and triangular, tapering in the ventral direction.

Of the three scapulocoracoid elements on each side of the skeleton, only the scapulae and the left anterior coracoid are preserved (Fig. 10). The left scapula is nearly complete, and connected by a suture to the incomplete left anterior coracoid. The scapula is similar to that of *Titanophoneus* (Orlov, 1958:figs. 41, 42). The blade of the scapula is laterally bowed, elongated, constricted in the middle of its length, and enlarged at the dorsal end. Several fine striations run along the external surface of the blade, extending from the ventral edge towards the dorsal one. The posteroventral portion of the scapula, which contributes to the glenoid, is not preserved. Only the convex anterior margin of the anterior coracoid is exposed, but the medial surface of this element is concave. The suture between the scapula and the anterior coracoid is covered by the left clavicle and the interclavicle.

TAXONOMY AND ONTOGENY OF *SINOPHONEUS YUMENENSIS*

When Cheng and Li (1997) named *Stenocybus acidentatus*, they did not directly compare their new taxon with *Sinophoneus yumenensis*, but they considered *Stenocybus* to be so different from Anteosauridae that they erected a new family for the former. Later, in the course of a study on the taxonomy of *Biarmosuchus*, Ivakhnenko (1999) proposed that *Stenocybus* might represent a juvenile form of *Sinophoneus*. Kammerer (2011) recently made detailed remarks on the various diagnoses that had been formulated for *Stenocybus*, and formally proposed that *Stenocybus* was a junior synonym of *Sinophoneus*. I agree with this conclusion and consider the material attributed to *Stenocybus* to represent part of the ontogenetic series available for *Sinophoneus*.

One distinct ontogenetic change involves pachyostosis of the skull. No distinct pachyostosis is present in small specimens, but the bones surrounding the orbit are pachyostosed in the holotype of *Sinophoneus* (GMV 1601). The median ridge on the skull roof is faint in the smallest known specimen (IVPP V18117), but a pair of bosses is present on the midline of the interorbital region. The ridge extends from the parietal foramen to a point only slightly beyond the orbit in specimen IVPP V18120, but extends further and is more distinct in the holotype of *Sinophoneus* (GMV 1601).

In order to quantify the ontogenetic changes seen in this species, a number of measurements were taken (Table 1). The accuracy of some of the measurements was affected by distortion, but the measurements nevertheless give a clear picture of the major changes in skull proportions that occurred through ontogeny. There is a gap in size and morphology between the holotype of *Sinophoneus* (GMV 1601) and the second-largest specimen, but the holotype falls on the growth trajectory defined by the small individuals.

The external naris and orbit increase only slightly in absolute size through ontogeny, showing strong negative allometry. By contrast, the temporal fenestra shows positive allometry, especially with regard to its height. The temporal fenestra is triangular and much smaller than the orbit in small specimens such as IVPP V18117, close to the size of the orbit in mid-sized specimens such as IVPP V18119; and much larger than the orbit in the holotype. The allometric expansion of the temporal fenestra is probably related to an increased ability to generate bite force, possibly indicating that adults and juveniles pursued different prey types.

Kammerer (2011) redefined the distinction between terminal and nonterminal positions of the external naris with regard to the distance between this structure and the alveolar margin of the premaxilla. This definition is problematic because of the strongly negative allometric growth of the external naris and its position close to the dorsal margin of the snout. This condition is observed not only in this species but also *Titanophoneus potens* (Orlov, 1958) and *Biarmosuchus tener* (pers. observ.). The position of the external naris could easily be miscoded in a nonadult individual. I prefer to define the position of the external naris according to its longitudinal position relative to the canine, even if this criterion would result in variable codings for *Anteosaurus* as mentioned by Kammerer (2011).

The skull increases remarkably in palatal width during ontogeny, as is shown by the distinct positive allometry of transverse process width relative to skull length (>1.4). By contrast, skull height is negatively allometric relative to skull length (<0.8). Accordingly, the skull is quite narrow and high in small specimens, but wide and relatively low in large ones. Because of the relative lengthening of the snout and lowering of the overall skull height in larger individuals, the snout profile is relatively straight in the holotype.

PHYLOGENETIC POSITION OF *SINOPHONEUS YUMENENSIS*

Sinophoneus yumenensis, when first named, was referred to Anteosauridae (Cheng and Ji, 1996). Although the new family Stenocybusidae (correctly emended to Stenocybidae by Ivakhnenko, 1999) was erected for *Stenocybus*, Kammerer (2011) showed *Stenocybus* to be a junior synonym of *Sinophoneus*, and also suggested that *Sinophoneus* is a derived anteosaur. However, *Sinophoneus* does not appear to have all five of the unambiguous synapomorphies of anteosaurs identified by Kammerer (2011). The vomers are poorly preserved in the holotype and not exposed in most specimens, but raised, elongated edges do not seem to be present based on IVPP V18119 and V12008. No ridge is present on the suture between the jugal and the lacrimal. *Sinophoneus* shares some primitive features with *Archaeosyodon*: naris anterior to canine, numerous teeth on palatal ramus of pterygoid, extensive teeth on transverse process of pterygoid, and prefrontal extends anteriorly beyond lacrimal. These characters indicate that *Sinophoneus* is more primitive than other anteosaurs. Kammerer (2011) viewed the holotype of *Sinophoneus* as lacking palatal teeth, but this could reflect poor preservation. In fact, no teeth of any kind are present in this specimen.

To explore the phylogenetic position of *Sinophoneus*, I modified the character lists and data matrices of Kammerer (2011) and Cisneros et al. (2012), and recoded some characters (Supplementary Data). The analysis was run in PAUP (Swofford, 2001) with all characters having equal weights, using the heuristic search algorithm, branches collapsed if maximum branch length is zero. One most parsimonious tree of length 83 steps was recovered (Fig. 11), with a consistency index (CI) of 0.60, a retention index (RI) of 0.73, and a rescaled consistency index (RC) of 0.44. This result is almost identical to that of Cisneros et al. (2012) other than in the position of *Sinophoneus* as the basal-most anteosaurid dinocephalian rather than a derived one, and in the position of *Microsyodon* as the sister taxon of *Australosyodon*. The synapomorphies of anteosaurid dinocephalians recovered in the present analysis include incisors with weak lingual heels; premaxillary alveolar margin canted anterodorsally; premaxilla forming broad, triangular palatal plate that separates anterior edge of vomers from incisor tooth row; quadrate rami of pterygoid intimately appressed, bifurcating anterior margin of basisphenoid; well-developed ornamentation on surfaces of lacrimal and maxilla; and crest extending from pineal foramen to orbit; postorbital bar with strong anteroventral curvature, so that temporal fenestra undercuts orbit. Even if the codings of some ontogenetical variable characters, such as characters 14, 16, and 38, are changed to 1, *Sinophoneus* still falls outside Anteosaurinae and emerges as a basal anteosaurid, although not the basal-most one. The same is true even if the ontogenetically variable characters are set to 1 and

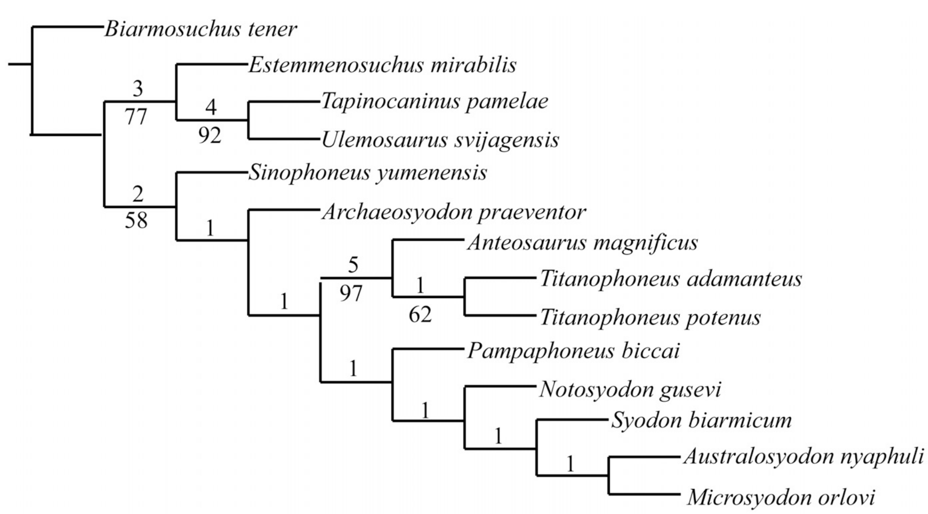

FIGURE 11. Cladogram of anteosaurid relationships. Decay indices and bootstrap values (above and below, respectively) are provided as measures of support for each node. Resampling calculated from 1000 replicates, and only values above 50% are shown.

'scroll-like' raised edges really are present on the vomers of *Sinophoneus*.

CONCLUSION

In this work, I describe the osteological features of *Sinophoneus yumenensis* based on previously described specimens and several new ones; confirm that *Stenocybus acidentatus* is a junior synonym of *Sinophoneus yumenensis*; and discuss ontogenetic variation in some cranial characters. Based on new observations, the relationships within Anterosauridae are reanalyzed. *Sinophoneus* falls outside Anteosaurinae and the revised phylogenetic analysis recovers this genus as the most basal known anteosaurid.

ACKNOWLEDGMENTS

I thank J.-L. Li for allowing me studying these specimens, H. Zhang and Z. Wang for preparing the specimens, J. Huang and Y. Wang for illustrations, C. Sullivan for improving the writing, and C. Kammerer, J. C. Cisneros, and B. Rubidge for critical review. NSFC grant 40972014 and 973 project 2012CB821902 supported this research.

LITERATURE CITED

Boonstra, L. D. 1954. The cranial structure of the titanosuchian: *Anteosaurus*. Annals of the South African Museum 42:108–148.

Boonstra, L. D. 1962. The dentition of the titanosuchid dinocephalians. Annals of the South African Museum 46:57–112.

Boonstra, L. D. 1968. The braincase, basicranial axis and median septum in the Dinocephalia. Annals of the South African Museum 50:195–273.

Broom, R. 1905. On the use of the term Anomodontia. Records of the Albany Museum 1:266–269.

Cheng, Z., and S. Ji. 1996. First record of a primitive anteosaurid dinocephalian from the Upper Permian of Gansu, China. Vertebrata PalAsiatica 34:123–134.

Cheng, Z., and J. Li. 1997. A new genus of primitive dinocephalian—the third report on Late Permian Dashankou lower tetrapod fauna. Vertebrata PalAsiatica 35:35–43.

Cisneros, J. C., F. Abdala, S. Atayman-Güven, B. S. Rubidge, A. M. C. Şengör, and C. L. Schultz. 2012. A carnivorous dinocephalian from the Middle Permian of Brazil and tetrapod dispersal in Pangaea. Proceedings of the National Academy of Science of the United States of America 109:1584–1588.

Ivakhnenko, M. F. 1999. Biarmosuches from the Ocher Faunal Assemblage of Eastern Europe. Paleontological Journal 33:289–296.

Ivakhnenko, M. F. 2003. Eotherapsids from the East European Placket (Late Permian). Paleontological Journal 37:S339–S465.

Kammerer, C. F. 2011. Systematics of the Anteosauria (Therapsida: Dinocephalia). Journal of Systematic Palaeontology 9:261–304.

Langer, M. C. 2000. The first record of dinocephalians in South America. Late Permian (Rio do Rasto Formation) of the Paraná basin, Brazil. Neues Jahrbuch für Geologie und Paläontologie, Abhandlungen 215:69–95.

Lepper, J., M. A. Raath, and B. S. Rubidge. 2000. A diverse dinocephalian fauna from Zimbabwe. South African Journal of Science 96:403–405.

Li, J. 2001. The most primitive lower tetrapod fauna in China. Science in China (Series D) 44:47–51.

Li, J., B. S. Rubidge, and Z. Cheng. 1996. A primitive anteosaurid dinocephalian from China—implications for the distribution of earliest therapsid faunas. South African Journal of Science 92:252–253.

Liu, J., Q.-H. Shang, K.-Q. Sun, and L. Li. 2012. The vertebrate fossil-bearing horizon in Yuman, Gansu and the Permian-Triassic strata in north Qilian area. Vertebrata PalAsiatica 50:373–381.

Orlov, Y. A. 1958. Carnivorous dinocephalians from the fauna of Ishev (Titanosuchia). Trudy Paleontologischeskogo Instituta AN SSSR 71:1–114.

Romer, A. S., and L. I. Price. 1940. Review of the Pelycosauria. Special Paper of the Geological Society of America 28:1–538.

Rubidge, B. S. 1994. *Australosyodon*, the first primitive anteosaurid dinocephalian from the Upper Permian of Gondwana. Palaeontology 37:579–594.

Seeley, H. G. 1894. Researches on the structure, organisation, and classification of the fossil Reptilia. Part IX., Section 1. On the Therosuchia. Philosophical Transactions of the Royal Society of London, Series B 185:987–1018.

Sigogneau-Russell, D., and A.-L. Sun. 1981. A brief review of Chinese synapsids. Geobios 14:275–279.

Simon, R., C. Sidor, K. Angielczyk, and R. Smith. 2010. First record of a tapinocephalid (Therapsida: Dinocephalia) from the Ruhuhu Formation (Songea Group) of southern Tanzania. Journal of Vertebrate Paleontology 30:1289–1293.

Swofford, D. L. 2001. PAUP*. Phylogenetic Analysis Using Parsimony (*And Other Methods), version 4.0b10. Sinauer Associates, Sunderland, Massachusetts.

Young, C.-C. 1979. A Late Permian fauna from Jiyuan, Henan. Vertebrata Palasiatica 17:99–113.

Submitted January 5, 2012; revisions received January 28, 2013; accepted February 18, 2013.
Handling editor: Bruce Rubidge.